Near-Infrared Luminescence Spectroscopy of Cobaltocene Doped into Single Crystals of Ruthenocene

Martin J. Davis and Christian Reber*

Département de chimie, Université de Montréal, Montréal, Québec, Canada H3C 3J7

Received June 28, 1994[⊗]

Near-infrared luminescence was observed from cobaltocene molecules doped into single crystals of ruthenocene. The spectrum and lifetime of the luminescence under UV excitation were studied between 6 and 100 K. Below 30 K, the cobaltocene luminescence is weak compared to that of the ruthenocene host lattice but becomes dominant above 50 K, evidence for a thermally induced energy transfer from ruthenocene to cobaltocene. The activation energy is estimated to be 140(40) cm^{-1} from luminescence decay curves. Selective excitation revealed the cobaltocene luminescence to be a broad, unstructured but highly asymmetric band with a maximum at 13 100 cm^{-1} (760 nm). Comparison with the absorption spectrum determines the energy of the lowest excited state to be 14 050 cm^{-1}. Calculated luminescence spectra using time-dependent quantum-mechanical calculations demonstrate that the highly asymmetric shape is due to a dynamic Jahn–Teller effect in the ground state along a high-frequency ligand-centered mode. The calculations also show an elongation of the Co–cyclopentadienyl bond length of 0.07 Å in the emitting state.

Introduction

Metallocenes are an extensively studied group of compounds which continue to form an active area of research. There has been renewed interest in first-row metallocenes and their derivatives, which have been shown to possess interesting synthetic and catalytic utility.[1,2] These properties often appear to depend on fine details of the structure and dynamics of the molecules. Many molecular ground state properties can be determined from luminescence spectra, but there are relatively few reports of luminescence spectra of metallocenes and even fewer detailed studies. One reason for this may be that any luminescence from first-row metallocenes is expected at relatively low energy, in the near-infrared, a technically difficult region of the spectrum. Other factors include the low quantum yield of the luminescence and problems of chemical stability of the compounds. However, for second- and third-row metallocenes, several luminescences have been reported,[3,4] making them useful as host lattices for first-row metallocenes. The best known example is ruthenocene, for which the highly structured luminescence spectrum has been analyzed in detail and excited state structural distortions have been determined.[5,6]

Cobaltocene is an air-sensitive metallocene with the $[Ar]3d^7$ electron configuration. It has been studied by a number of methods,[7–14] but to the best of our knowledge, no luminescence has ever been reported. The exact point group of the molecule in the solid state is C_i,[7] but EPR, vibrational, and electronic spectra have been successfully interpreted using a D_{5d} idealized symmetry.[10,13,14] We will adhere to this convention for the analysis of our spectra. Several investigations of the absorption spectrum of cobaltocene in solution and the solid state have been reported[11–14] as well as several electronic structure calculations of varying sophistication.[13–16] The ground state is $^2E_{1g}$ with the unpaired electron in an e_{1g} antibonding orbital, and therefore the metal–cyclopentadienyl (M–cp) bond is longer and weaker in cobaltocene than in ferrocene, which contains one less d electron.[17] The first absorption band in cobaltocene is due to the transition of an electron from an a_{1g} orbital to an e_{1g} orbital, leading to an $^2A_{2g}$ state.[14] Since the ground state is degenerate, it is possible that the molecule will exhibit a Jahn–Teller distortion. EPR measurements indicate that such an effect is indeed present, and it was suggested that the distortion was dynamic along an e_{2g} ligand stretching coordinate.[13]

The aim of this work is to identify luminescence from cobaltocene and to obtain, from the spectrum, information about the nature and structure of the electronic states involved. We used samples of cobaltocene doped into single crystals of ruthenocene in the hope that it might be possible to amplify any weak luminescence from cobaltocene by sensitization with the ruthenocene. In addition, quantitative information on energy transfer processes in organometallic solids is scarce in the literature but important for the understanding of excitation dynamics and intermolecular interactions in these systems.

Experimental Section

Cobaltocene and ruthenocene were obtained from Strem Chemicals and were purified by sublimation in sealed tubes. Cobaltocene is very

[⊗] Abstract published in *Advance ACS Abstracts,* July 15, 1995.

(1) Foucher, D. A.; Tang, B. Z.; Manners, I. *J. Am. Chem. Soc.* **1992**, *114*, 6246.
(2) Nelson, J. M.; Rengel, H.; Manners, I. *J. Am. Chem. Soc.* **1993**, *115*, 7035.
(3) Lees, A. J. *Chem. Rev.* **1987**, *87*, 711.
(4) Perutz, R. *Chem. Soc. Rev.* **1993**, 361.
(5) Crosby, G. A.; Hager, G. D.; Hipps, K. W.; Stone, M. L. *Chem. Phys. Lett.* **1974**, *28*, 497.
(6) Hollingsworth, G. J.; Shin, K.-S. K.; Zink, J. I. *Inorg. Chem.* **1990**, *29*, 2501.
(7) Bünder, W.; Weiss, E. *J. Organomet. Chem.* **1976**, *92*, 65.
(8) Almenningen, A.; Gard, E.; Haaland, A.; Brunvoll, J. *J. Organomet. Chem.* **1976**, *107*, 273.
(9) Eicher, H.; Köhler, F. H. *Chem. Phys.* **1988**, *128*, 297.
(10) Gächter, B. F.; Koningstein, J. A.; Aleksanjan, V. T. *J. Chem. Phys.* **1975**, *62*, 4628.
(11) Gordon, K. R.; Warren, K. D. *Inorg. Chem.* **1978**, *17*, 987.
(12) Barton, T. J.; Grinter, R.; Thomson, A. J. *J. Chem. Soc., Dalton Trans.* **1979**, 1912.
(13) Ammeter, J. H.; Swalen, J. D. *J. Chem. Phys.* **1972**, *57*, 678.
(14) Weber, J.; Goursot, A.; Pénigault, E.; Ammeter, J. H.; Bachmann, J. *J. Am. Chem. Soc.* **1982**, *104*, 1491.
(15) König, E.; Schnakig, R.; Kremer, S.; Kanellakopulos, B.; Klenze, B. *Chem. Phys.* **1978**, *27*, 331.
(16) Famiglietti, C.; Baerends, E. J. *Chem. Phys.* **1981**, *62*, 407.
(17) Haaland, A. *Acc. Chem. Res.* **1979**, *12*, 415.

0020-1669/95/1334-4585$09.00/0

sensitive to oxidation, so all manipulations involving it were carried out under a dry argon atmosphere in a glovebox or in sealed tubes.

Doped crystals were prepared by cosublimation of ruthenocene and cobaltocene.[13] In a typical preparation, 200 mg of ruthenocene and 2 mg of cobaltocene were placed in a glass tube which was then sealed under a vacuum of about 10^{-5} Torr. The tube was then lowered into a bath maintained at 80 °C at a rate of 0.6 mm/h over a period of 1 week. The doped crystals were formed by repeated sublimation and crystallization in progressively higher parts of the tube, thus contributing to the purification of the final crystals. The resulting crystals were approximately cuboid and were up to about 2 mm in edge length. The colors ranged from pink to violet, with many crystals showing domains of both colors. No attempt was made to analyze the concentration of cobaltocene in the crystals since their evident inhomogeneity would render such results of very limited value. From the quantities of starting materials used and the estimated quantity of ruthenocene remaining in the bottom of the tube at the end of the crystallization, the average cobaltocene concentration may be estimated to be between 0.5 and 0.05% M.

For all spectroscopic investigations the samples were placed in a helium gas continuous-flow cryostat (Oxford Instruments CF 1204) with quartz windows. The temperature of the sample was determined by means of a Rh–Fe resistor on the sample holder. Spectroscopic measurements were always started at least 10 min after the required temperature, as indicated by the resistor, was attained. Absorption spectra were recorded using a Varian Cary 5E spectrometer.

The luminescence spectra with broad-band UV excitation were obtained using a spectrometer presented in the following. Their excitation source was a 150 W Xe arc lamp (ICL LX-150UV); the radiation was filtered through a 10 cm cell with quartz windows containing a 1 M copper sulfate solution to remove the IR radiation. The UV excitation was selected with a Schott UG11 filter and focused onto the sample using quartz lenses. A spherical mirror served to collect the luminescence perpendicular to the excitation and to focus it onto the entrance slit of a Spex 1800-II monochromator. A long-pass filter, either a Schott KV450 or RG610 depending on the spectral range to be examined, was placed in front of the entrance slit of the monochromator which was equipped with a 1200 line/mm grating with a blaze wavelength of 500 nm. The detection system consisted of either a Hamamatsu R4632 photomultiplier connected to a Stanford Research SR400 photon counter or a cooled Hamamatsu R406 photomultiplier connected to a Stanford Research SR510 lock-in amplifier. In the latter case, an optical chopper (Stanford Research SR540) was placed in front of the monochromator entrance slit. The amplifiers were interfaced to a personal computer where the data were collected using software written in our laboratory and the MS-DOS operating system.

A second system was also used for recording luminescence spectra, similar to that described above but with the following differences. The excitation source was the 514.5 nm line of a Coherent Innova CR-12 argon ion laser. The monochromator was a Spex 500M equipped with a 600 line/mm, 1 μm blaze grating and controlled with an MSD2 controller interfaced to the computer. Input to the photon counter was taken from a cooled Hamamatsu R928 photomultiplier amplified by a factor of 5 using a Stanford Research SR440 preamplifier.

Luminescence decay curves were obtained using the optical equipment and detectors of the second luminescence system. However, the excitation source was a Lumonics HyperEx-400 XeCl excimer laser giving pulses at 308 nm of less than 50 ns duration. The output from the photomultipliers, amplified by a factor of 5 with the SR440 for the R406 photomultiplier, was terminated at 300 Ω and connected to a 500 MHz Hewlett Packard HP54503A digital oscilloscope. The oscilloscope was set to average 2048 pulses.

The alignment of the monochromators was controlled with a helium–neon laser. Wavelength calibration was checked using mercury and neon discharge lamps.

Since the detector sensitivities vary greatly over the wavelength range of the emission, all luminescence spectra were corrected for system response in the following manner. The spectra of a 50 W tungsten–halogen lamp and an Oriel 63350 calibrated light source were measured under the same experimental conditions and were found to be almost identical. Both spectra were found to be very close to that of a blackbody at a temperature of 3000(±100) K. The spectrum of the 50 W lamp was then recorded using exactly the same experimental conditions as for the luminescence spectra. For this it was necessary to place a neutral density filter with a known absorption spectrum before the monochromator entrance slit. Correcting for the filter absorption and dividing by the blackbody curve gave the relative spectral response of the system. All corrections were performed in the wavelength domain before converting to a wavenumber scale.[18]

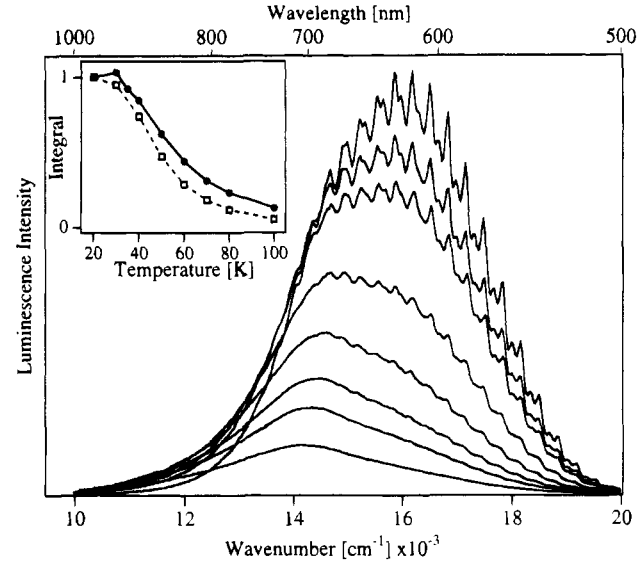

Figure 1. Luminescence spectra of doped crystals under UV excitation. Spectra recorded at 20, 35, 40, 50, 60, 70, 80, and 100 K are shown (top to bottom). The inset shows the integrated intensity of the spectra as a function of temperature (filled circles) compared to integrated intensities measured for pure ruthenocene (open squares).

Luminescence decay rate constants (k) were calculated from the luminescence decay curves by fitting an exponential function, Ae^{-kt}, to the portion of the curve below 60% of the peak intensity. A commercial least-squares fitting routine was used.[19]

Calculations of spectra were performed using software, described elsewhere,[20,21] running on a Silicon Graphics 4D/380 computer. These calculations generally used a space grid of 512 points with a separation of 2.35×10^{-3} Å and 500 time steps with a separation of 2 fs and required about 20 s of CPU time for execution. Using twice the number of points on the space grid and twice as many time steps did not alter the calculated spectra, indicating that the grids used were sufficiently fine to avoid significant numerical errors.

Spectroscopic Results

The luminescence spectra of cobaltocene doped into ruthenocene at different temperatures are shown in Figure 1. At the lowest temperatures we observe a structured spectrum similar to the emission band of pure ruthenocene reported in the literature.[5,6] A detailed comparison of a high-resolution spectrum of the doped single crystal at 20 K and the spectrum of a single crystal of pure ruthenocene measured on our instrument is shown in Figure 2. The spectrum of pure ruthenocene is identical to those in the literature. The doped crystal showed a slight shift of the highest energy vibronic peaks by 20 cm^{-1} to lower energy, probably as a consequence of the slightly different crystal structure caused by the doping. More importantly, the luminescence band maximum observed for the doped crystal at 20 K is at 16 100 cm^{-1}, lower by 600 cm^{-1} than that for pure ruthenocene, and the overall width at half-height is 3700 cm^{-1}, larger than the width of 3000 cm^{-1} observed for pure

(18) Ejder, E. *J. Opt. Soc. Am.* **1969**, *59*, 223.
(19) The fitting routine of the Igor Pro data analysis package by Wavemetrics Inc. was used.
(20) Reber, C.; Zink, J. I. *Comments Inorg. Chem.* **1992**, *13*, 177.
(21) Kosloff, D.; Kosloff, R. *J. Comput. Phys.* **1983**, *52*, 35.

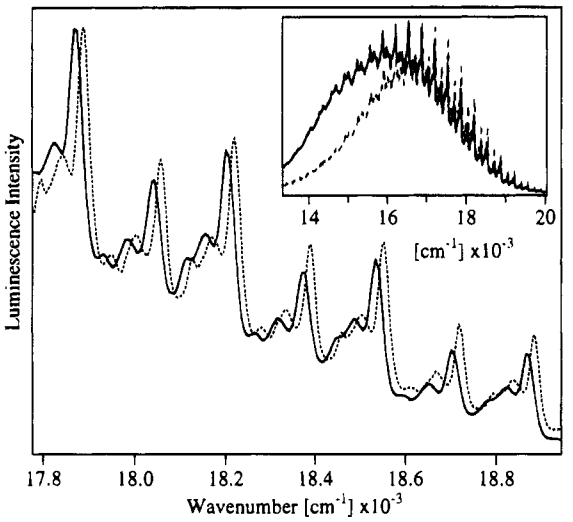

Figure 2. High-resolution luminescence spectra at 20 K. The main figure shows a portion of the spectrum of the doped crystals (solid line) compared to the same portion of the spectrum of pure ruthenocene (dashed line). The spectral resolution is not instrument limited. The inset shows the corresponding complete spectra.

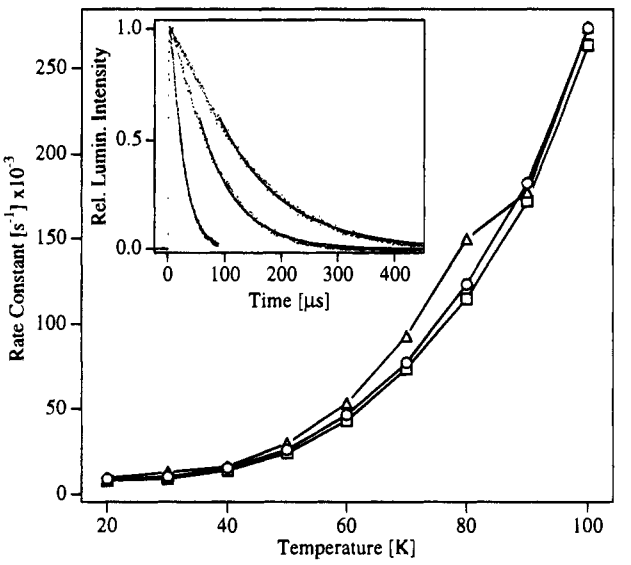

Figure 3. Rate constants for luminescence decay measured for doped crystals at 550 nm (circles) and 850 nm (triangles) and for pure ruthenocene at 550 nm (squares). The inset shows luminescence decay curves for the doped crystals at 550 nm (points) recorded at 20, 40 and 60 K together with exponential fits (lines) to the data.

ruthenocene. These important differences indicate that luminophores other than the host ruthenocene molecules contribute to the observed spectrum, even at the lowest temperatures.

The luminescence spectrum shows important changes with temperature. First, the integrated luminescence intensity decreases with increasing temperature, as presented in the inset to Figure 1 for both doped and pure samples. They show a very similar decrease of intensity with temperature. The most important change concerns the shape of the spectrum. As seen in Figure 1, the band maximum for the doped crystal shifts from 16 100 cm^{-1} at 20 K to 14 200 cm^{-1} at 100 K, a dramatic change not observed for pure ruthenocene. It is obvious that this change corresponds to a thermally sensitized luminescence from a different luminophore, spectroscopically identified to be the cobaltocene molecule (see below). The energy transfer processes governing the shape of the luminescence spectrum will be examined in the first part of the discussion. The change of luminescence band shape was observed with four different samples (obtained from different batches of starting materials), showing that the spectra reported in Figure 1 are reproducible. We note that samples of pure cobaltocene and heavily doped samples showed no luminescence under the same experimental conditions, most likely due to efficient energy transfer between cobaltocene molecules and deactivation at deep traps, possibly associated with cobaltocenium molecules. In addition, it was found that a sample no longer showed the near-infrared luminescence after being left in the air for several days. This is most likely due to oxidation of the cobaltocene and provides further evidence that this luminescence indeed originates from cobaltocene molecules.

Figure 3 shows luminescence decay rate constants as a function of temperature, again for both cobaltocene doped into ruthenocene and pure ruthenocene crystals. For the doped crystals, measurements of the luminescence decay were made at 550 and 850 nm. At the first wavelength, luminescence from the ruthenocene host dominates the spectrum, while at the second wavelength we observe only the decay characteristics of cobaltocene. For pure ruthenocene the measurements were made at 550 nm and the results obtained are in agreement with values reported in the literature.[5,6] The inset to Figure 3 shows some examples of measured decay curves together with exponential fits (solid lines). The observed luminescence decay curves generally showed a region just after the laser pulse with

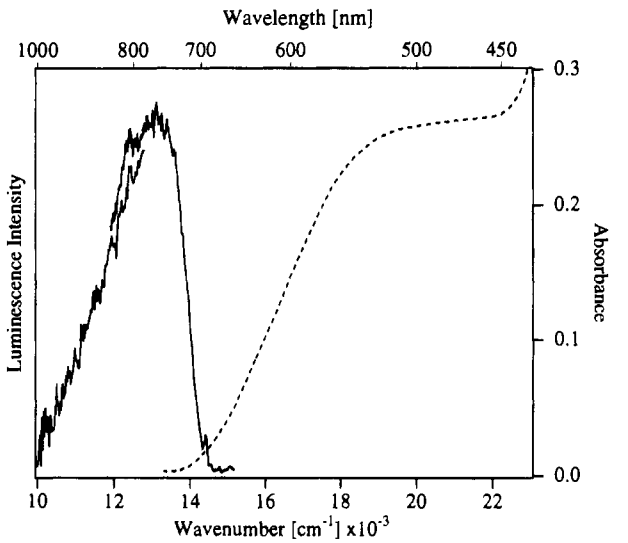

Figure 4. Luminescence and absorption spectra of doped crystals. The solid line shows the luminescence spectrum at 6 K using 514.5 nm laser excitation. The portion of the luminescence at higher energy was obtained using an R928 photomultiplier tube while the portion at lower energy was recorded using an R406 photomultiplier tube and is slightly offset along the intensity axis for clarity. The dashed line shows the absorption spectrum at 80 K.

a decay somewhat slower than that predicted by a single-exponential function. This nonexponential region is probably the result of some fast energy transfer processes among the ruthenocene molecules. The curves did not show an excessively steep decay after the pulse, often characteristic of laser heating of the sample. We fitted only the part of the curves with intensities lower than 60% of the maximum intensity after the pulsed laser excitation in order to prevent the fast energy transfer processes disturbing the single-exponential fits. In the region of the curves used for the fits, the agreement between fit and experiment is excellent. Measurements at several temperatures on a second sample gave similar rates.

Figure 4 shows the luminescence spectrum of a doped crystal at 6 K, excited with the 514.5 nm line of an argon ion laser. The observed band is broad and highly asymmetric with a maximum at 13 100 cm^{-1}. The spectrum was recorded using

different detectors for the high- and low-energy spectral regions, and the similarity of the spectra in the overlapping region is a good indication of the high quality of the system response corrections used. At the excitation wavelength, only the cobaltocene molecules will absorb, since the electronic origin for the lowest energy transition of ruthenocene is at higher energy.[22] This selective excitation allows us to separate the luminescence spectrum of cobaltocene from the spectrum of the ruthenocene host lattice. The intensity of the spectrum is much lower than that for the sensitized luminescence observed in the same wavelength range, illustrating the efficient energy transfer from the host lattice which we use to amplify the weak signal from the guest molecules. The band shape of the cobaltocene luminescence spectrum will be analyzed in the second part of the discussion. The comparison of absorption and luminescence spectra in Figure 4 clearly shows that the infrared luminescence originates from cobaltocene molecules: the spectra show a slight overlap at the electronic origin, and the onset of the first absorption band and the band maximum are identical to those of literature absorption spectra for both cobaltocene doped into ruthenocene and pure cobaltocene.[13,14] The absorption spectrum contains much less information on the lowest energy transition because several excited states are in the energy range of the first band, leading to a broad, featureless spectrum. The combination of absorption and luminescence spectra allows us to determine the energy of the lowest excited state of cobaltocene as 14 050 cm^{-1}. The large Stokes shift of 5500 cm^{-1} estimated from Figure 4 suggests that there are significant structural differences between the ground and emitting states.

Discussion

(a) Energy Transfer from Ruthenocene to Cobaltocene. The luminescence spectra in Figure 1 clearly show that there is a thermally activated transfer of energy from excited ruthenocene molecules to ground state cobaltocene molecules, since the low-energy band increases in intensity relative to the high-energy band on increasing the temperature. We discuss this energy transfer in terms of a simple model in which an excited ruthenocene molecule either decays directly to the ground state by radiative or nonradiative relaxation or excites a cobaltocene molecule by a nonradiative energy transfer process. The cobaltocene molecules then decay to the ground state either radiatively or nonradiatively. The rate constant for the total direct de-excitation of ruthenocene is k_a, that for cobaltocene is k_b, and the rate constant for the nonradiative energy transfer is k_{ab}.

This model contains several considerable simplifications. First, it takes no account of energy transfer between ruthenocene molecules. Second, it is probable that there is considerable radiative energy transfer from ruthenocene to cobaltocene, given the favorable overlap between the luminescence spectrum of the former and the absorption spectrum of the latter (compare Figures 1 and 3). These radiative energy transfer processes are not included in the model. Last, it is to be expected that some cobaltocene molecules will be directly excited, since they absorb strongly in the UV, but this effect is also neglected in the model. However, it should be noted that the last two phenomena will have no effect on the luminescence decay curves of ruthenocene measured at 550 nm, only on those of cobaltocene at 850 nm. The first effect is likely to be most important directly after excitation when the ruthenocene luminescence is still relatively intense and seems to be apparent in the experimental curves as noted in the previous section. The procedure for determining the decay rate constants was designed to minimize this influence.

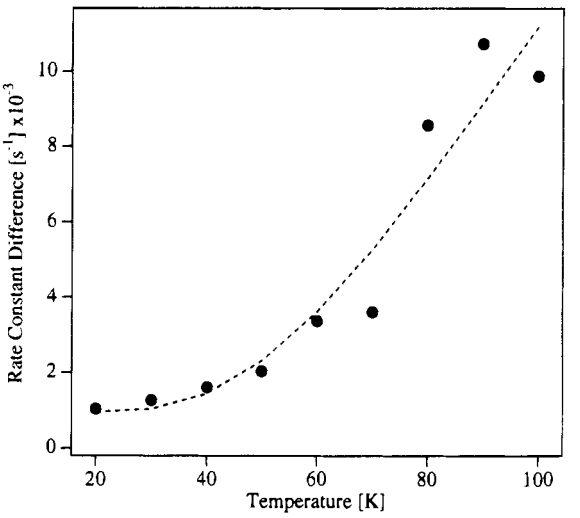

Figure 5. Difference in luminescence decay rate constants between the doped crystals and pure ruthenocene at 550 nm. The dashed line shows the results of a fit to the points, explained in the text.

First, it will be assumed that k_a is the same for the doped material as for pure ruthenocene. This is supported by the similar decrease in overall luminescence intensity with temperature observed for the two materials, shown in Figure 1, together with the identical luminescence decay rate constants at low temperatures, which indicate that the absolute luminescence intensities are comparable. It follows from this assumption that the difference in the observed rate of luminescence decay for ruthenocene in the two materials is due to the energy transfer to cobaltocene in the doped sample. The rate constants k_{ab} can thus be calculated as the differences in rate constants for the luminescence decay in the two materials. They are subject to considerable error but nevertheless show a fairly consistent increase in k_{ab} with temperature, as presented in Figure 5. A fit to these values using the equation $k_{ab}(T) = k_0 + A \exp(-\Delta E/kT)$ was moderately successful and yielded an activation energy barrier for the energy transfer, ΔE, of 140(40) cm^{-1}. The fitted curve is shown as a dashed line in Figure 5. The constant, k_0, represents an energy transfer mechanism without an activation energy barrier. Its numerical value of 948(810) s^{-1} obtained from the fit carries a large error, and we will not attempt to interpret it with our model. The value of 77(47) $\times$ 10^3 s^{-1} found for A is poorly determined due to the lack of data at high temperature but has little physical significance and will not be discussed further.

The luminescence decay curves measured for cobaltocene at 850 nm are expected to show a maximum at a time depending on the value of k_b relative to that of k_{ab}. The fact that no maximum in cobaltocene luminescence decay is observed at times greater than about 5 μs suggests a lower limit of approximately 10^6 s^{-1} for k_b. The decay curves at 850 nm are slightly nonexponential, being steeper at short times than at long times. This leads to somewhat higher decay rates calculated from a single-exponential fit than at 550 nm, a difference most likely due to the luminescence decay of directly excited cobaltocene centers.

In summary, the analysis of the luminescence spectra and lifetimes indicates that there is thermally activated energy transfer from ruthenocene to cobaltocene and allows the energy barrier to be estimated as 140 cm^{-1}. However, it is also clear that there are a number of additional energy transfer processes occurring in these doped crystals which cannot be analyzed quantitatively within our simple model.

(22) Riesen, H.; Krausz, E.; Luginbühl, W.; Biner, M.; Güdel, H. U.; Ludi, A. *J. Chem. Phys.* **1992**, *96*, 4131.

(b) Molecular Distortions of Cobaltocene Determined from the Luminescence Spectrum. The luminescence spectrum of cobaltocene in Figure 4 allows us to determine the normal coordinates along which distortions occur. In this section, we will characterize the electronic ground state and the lowest energy excited state of cobaltocene on the basis of our luminescence spectrum and literature results obtained for cobaltocene with different physical methods. Due to the lack of resolved vibronic structure, our analysis will be less straightforward than the one for the emission spectrum of ruthenocene, a textbook example of a resolved spectrum. We will use EPR and vibrational spectroscopic results from the literature to independently determine some of the parameters used in the analysis of the spectrum.

The luminescence and absorption spectra shown in Figure 4 clearly determine the energy of the lowest excited state of cobaltocene as 14 050 cm^{-1}. This is the first time that the energy of the emitting state of this molecule has been determined experimentally. Electronic structure calculations in the literature[14] predict the lowest energy excited state at 15 300 cm^{-1}, in good agreement with our spectroscopic findings. The ground and lowest energy excited states are $^2E_{1g}$ and $^2A_{2g}$, respectively, in D_{5d} symmetry. The degenerate $^2E_{1g}$ ground state is susceptible to a Jahn–Teller effect, as demonstrated by EPR spectroscopy. No such effect can be expected for the nondegenerate excited state, indicating that all distortions along non-totally-symmetric coordinates must occur in the ground state.

For the calculations of emission spectra we use Heller's time-dependent theory of electronic spectroscopy described in detail elsewhere.[23] We use the computer implementations outlined in refs 20 and 21. The method is equivalent to a standard Franck–Condon analysis for harmonic potential energy surfaces but can be easily generalized to degenerate states and nonharmonic potential energy surfaces, a very powerful tool for the understanding of the spectra of metallocenes. Only the normal coordinates along which a distortion between initial and final potential energy surfaces occurs need be included in the model.

The emission intensity is given as

$$I_{lum}(\omega) = C\omega^3 \int_{-\infty}^{+\infty} \exp(i\omega t)\left\{\langle\phi|\phi(t)\rangle \exp\left(-\Gamma^2 t^2 + \frac{iE_0}{\hbar}t\right)\right\} dt \quad (1)$$

The main ingredient of the calculation is the evolution of a wavepacket with time on the final potential energy surface of the transition. We calculate its autocorrelation, $\langle\phi|\phi(t)\rangle$, whose Fourier transform to the frequency domain gives the calculated spectrum. E_0 denotes the energy of the electronic origin transition, and Γ is a phenomenological damping factor, determining the width of each transition forming the vibronic structure.

A technical advantage of the time-dependent theoretical approach is that different normal coordinates can be considered separately, their autocorrelations multiplied, and the result Fourier-transformed to give the full spectra. We therefore need to propagate only one-dimensional wavefunctions along the normal coordinates that show a distortion and can calculate the total autocorrelation with

$$\langle\phi|\phi(t)\rangle = \prod\langle\phi_i|\phi_i(t)\rangle \quad (2)$$

In order to keep the number of parameters in our model to a minimum, we chose harmonic potential energy surfaces to represent the initial and final states of the electronic transition.

(23) Heller, E. J. *Acc. Chem. Res.* **1981**, *14*, 368.

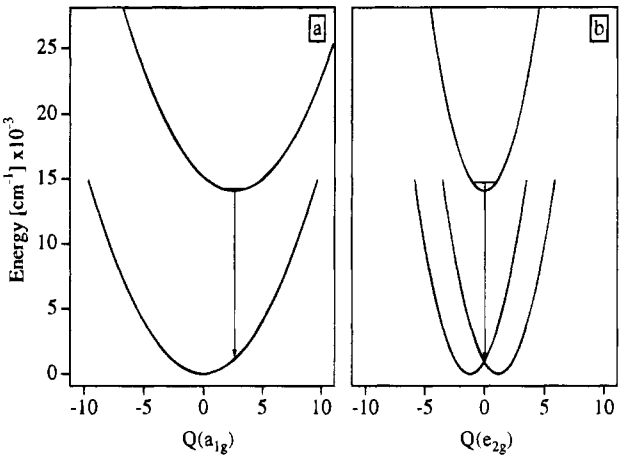

Figure 6. Potential energy surfaces used for the calculation of luminescence spectra: (a) Co–cp stretching mode; (b) high-frequency, ligand-centered mode. The first energy level is shown on each of the excited state surfaces, and the luminescence transition is shown schematically by the arrows.

This functional form of the potential energy surfaces is not a fundamental limitation of the computational method. The potential energy surfaces along dimensionless normal coordinates are defined by their vibrational energies k_i in cm^{-1} and the offset of their minimum by ΔQ_i from the origin of the abscissa:

$$V_i(Q) = {}^1/_2 k_i (Q - \Delta Q_i)^2 \quad (3)$$

This equation is used for the potential energy along nondegenerate vibrational coordinates in both the ground and excited states. The electronic ground state of cobaltocene shows distortions along a degenerate vibration. For this situation we use a simplified model based on two coupled diabatic surfaces, each represented by eq 3. The evolution of the wavepacket with time needs to be calculated on both coupled diabatic surfaces simultaneously.[25] The split-operator formalism of Feit and Fleck[24] is used for these calculations.

We start from the assumption that a significant bond length change between ground and emitting states occurs along the totally symmetric (a_{1g}) Co–cp stretching normal coordinate. This is the largest structural change observed in ruthenocene,[6] and the vibrational frequency of this mode in pure cobaltocene is 320 cm^{-1}, determined from Raman spectra.[10] We use this frequency for both electronic states involved in the transition. This simple, one-dimensional model, corresponding to the potential energy surfaces shown in Figure 6a, leads to unsatisfactory agreement between calculated and experimental spectra, as illustrated by the dashed line in Figure 7. We therefore need to add a second coordinate to our model. It is clear from the asymmetric shape of the experimental spectrum that the second vibrational mode has to have a much higher frequency than the Co–cp stretching mode. Detailed EPR measurements in the literature suggest a dynamic Jahn–Teller effect in the ground electronic state of cobaltocene, with a ligand-centered C–C stretching mode of e_{2g} symmetry as the active mode.[13] Its frequency was reported to be 1356 cm^{-1} for ferrocene, and we use this value in our calculations. A distortion along this mode lowers the symmetry of the molecule, but since the effect

(24) Feit, M. D.; Fleck, J. A., Jr.; Steiger, A. *J. Comput. Phys.* **1982**, *47*, 412.
(25) Zhang, J.; Heller, E. J.; Huber, D.; Imre, D. G. *J. Phys. Chem.* **1991**, *95*, 6129.
(26) Longuet-Higgins, H. C.; Öpik, U.; Pryce, M. H. L.; Sack, R. A. *Proc. R. Soc. London, Ser. A* **1958**, *244*, 1.

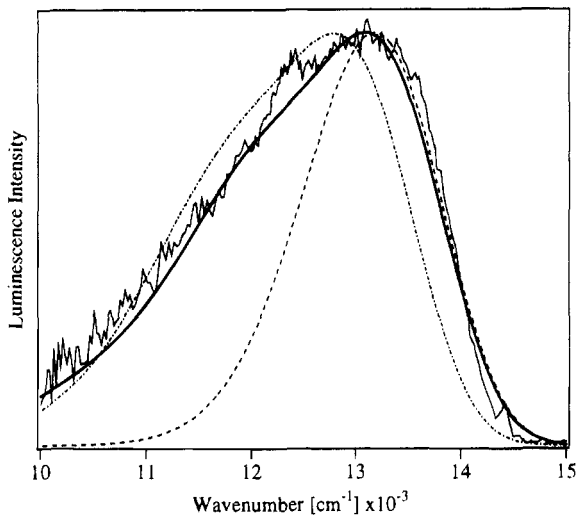

Figure 7. Calculated and experimental luminescence spectra of cobaltocene. The heavy solid line shows the best calculated spectrum obtained. The dashed line shows the best calculated spectrum obtained by considering the a_{1g} mode distortion only (Figure 6a). The dotted–dashed line shows the best spectrum obtained using a coupling of 300 cm^{-1} between the e_{2g} mode diabatic surfaces.

is dynamic, no static distortion is observed by X-ray diffraction.[7] We include the Jahn–Teller effect in our model in a simplified form, illustrated by the potential energy surfaces in Figure 6b, reducing the $E_{1g} \times e_{2g}$ problem to one effective dimension. The reason for this simplified model is again our attempt to minimize the number of parameters but still keep the model physically meaningful. The lack of resolved vibronic structure does not allow us to discriminate between the full $E_{1g} \times e_{2g}$ problem and our simplified model. Besides the vibrational frequency and the positions of the potential energy minima, an additional parameter is the coordinate-independent coupling between the two diabatic surfaces of Figure 6b, V_{12}. Again, V_{12} is a simplified parameter, only qualitatively representing the true Jahn–Teller coupling of the full $E_{1g} \times e_{2g}$ problem.

The calculated spectrum using the two-dimensional model including both the totally symmetric stretching and the ligand-centered vibrations is shown as a solid line in Figure 7. The agreement between calculated and experimental spectra is excellent in view of the many simplifications of our model. Values of 0, 14 050, and 250 cm^{-1} were used for V_{12}, the energy of the electronic origin E_0, and the damping factor Γ, respectively. The calculations clearly show the presence of a distortion along a high-frequency mode, a situation very different from the case of ruthenocene, where the highest energy mode contributing to the emission spectrum has a vibrational energy of 445 cm^{-1}.[6] The coupling between the two diabatic surfaces is small or zero, as illustrated by the calculated spectrum in Figure 7 and indicating qualitatively that the true Jahn–Teller coupling in the full $E_{1g} \times e_{2g}$ problem is small. We include in Figure 7 a spectrum calculated with a coupling constant of 300 cm^{-1}, with the position of the potential energy minima adjusted to give the best fit. It is obvious that this fit is much less satisfactory than the calculated spectrum with a coupling constant of 0 cm^{-1}, limiting thus the physical range of the coupling parameter. The spectrum illustrates a rare situation of a Jahn–Teller effect with a mainly ligand-centered active mode, in contrast to the vast majority of examples for Jahn–Teller effects where metal–ligand modes are active. We expect similar effects in orbitally degenerate electronic states of other metallocenes because of an analogous coupling between the d electrons of the metal center and the η^5-bonded cyclopentadienyl ligand, where vibrational motion on the ligand directly influences the metal–ligand bonds and the d electrons of the metal. The potential energy surfaces obtained from our analysis with time-dependent theoretical methods illustrate that the Jahn–Teller effect in cobaltocene is dynamic, in agreement with the literature.[7,13]

The values for ΔQ_i obtained for the a_{1g} and e_{2g} modes are 2.61 and 1.18, along the dimensionless normal coordinates. These values correspond to Huang–Rhys parameters S_{a1g} and S_{e2g} of 3.4 and 0.7, respectively. Despite the low value for S_{e2g}, the Stokes shift is considerable, another consequence of the high vibrational energy of the e_{2g} mode. The a_{1g} distortion is converted to the normal coordinate in angstrom units[6] and, using the same definition of the coordinate as for ruthenocene, gives a difference in Co–cp bond length of 0.07 Å, a value significantly smaller than that for ruthenocene, where a distortion of 0.12 Å was determined.[6] This may be qualitatively rationalized by considering that excitation of ruthenocene leads to the population of a previously empty antibonding orbital whereas for cobaltocene this orbital is already occupied in the ground state. The distortion along the high-frequency e_{2g} mode cannot be easily converted to a structural distortion and, due to the dynamic nature of the Jahn–Teller effect, would not be a physically meaningful value.

New insight into the Jahn–Teller effect and molecular distortions in cobaltocene is obtained with the combination of our time-dependent theoretical model and the unresolved luminescence spectrum, a promising approach currently applied in our laboratories to other first-row metallocenes.

Acknowledgment. This work was made possible by research grants from the NSERC (Canada) and FCAR (Province of Quebec). We thank H. U. Güdel and J. H. Ammeter for making available samples for preliminary studies.

IC9407508